



Do model polymer therapeutics sufficiently diffuse through articular cartilage to be a viable therapeutic route?

Alison Powell, Bruce Caterson, Clare Hughes, Alison Paul, Craig James, Stephen Hopkins, Omar Mansour & Peter Griffiths

To cite this article: Alison Powell, Bruce Caterson, Clare Hughes, Alison Paul, Craig James, Stephen Hopkins, Omar Mansour & Peter Griffiths (2017) Do model polymer therapeutics sufficiently diffuse through articular cartilage to be a viable therapeutic route?, Journal of Drug Targeting, 25:9-10, 919-926, DOI: [10.1080/1061186X.2017.1378660](https://doi.org/10.1080/1061186X.2017.1378660)

To link to this article: <https://doi.org/10.1080/1061186X.2017.1378660>



© 2017 The Author(s). Published by Informa UK Limited, trading as Taylor & Francis Group



Accepted author version posted online: 11 Sep 2017.
Published online: 21 Sep 2017.



Submit your article to this journal [↗](#)



Article views: 34



View related articles [↗](#)



View Crossmark data [↗](#)

Do model polymer therapeutics sufficiently diffuse through articular cartilage to be a viable therapeutic route?

Alison Powell^a, Bruce Caterson^a, Clare Hughes^a, Alison Paul^b, Craig James^b, Stephen Hopkins^b, Omar Mansour^c and Peter Griffiths^c

^aSchool of Biosciences, Cardiff University, Cardiff, UK; ^bSchool of Chemistry, Cardiff University, Cardiff, UK; ^cDepartment of Pharmaceutical, Chemical and Environmental Sciences, Faculty of Engineering and Science, University of Greenwich, Kent, UK

ABSTRACT

The ability of a polymer therapeutic to access the appropriate subcellular location is crucial to its efficacy and is defined to a large part by the many and complex cellular biological and biochemical barriers such that a construct must traverse. It is shown here that model dextrin conjugates are able to pass through a cartilaginous extracellular matrix into chondrocytes, with little perturbation of the matrix structure, indicating that targeting of potential therapeutics through a cartilaginous extracellular matrix should be proven possible. Rapid chondrocytic targeting of drugs which require intra cellularisation for their activity and uniform extracellular concentrations of drugs with an extracellular target, is thus enabled through polymer conjugation.

ARTICLE HISTORY

Received 14 July 2017
Accepted 8 September 2017

KEYWORDS

Diffusion; neutron scattering; chondrocytic gels; polymer therapeutic; barrier

Introduction

Articular cartilage lines the load bearing joints of the body acting to reduce friction and absorb mechanical loads. It is an aneural, avascular, hypocellular tissue, composed of a dense extracellular matrix controlled and secreted by the chondrocytes within it. The chondrocytes comprise less than 2% of the volume of mature articular cartilage with the remainder comprising a highly organised network of collagen fibrils, proteoglycans and water. The matrix macromolecules of articular cartilage give the tissue its unique structure and function. These structural macromolecules include collagens (mainly type II), proteoglycans and non-collagenous proteins. The type II collagen fibril meshwork gives the cartilage its form and tensile strength. The proteoglycans and non-collagenous proteins of articular cartilage bind to the collagen meshwork or become mechanically entrapped within it. The major proteoglycan of articular cartilage is aggrecan, which has numerous glycosaminoglycan chains attached to its core protein and forms huge multimolecular aggregates with hyaluronan and a link protein. Hydration of the glycosaminoglycan chains of aggrecan provides cartilage with its compressibility functions.

More than ten million people in the UK have long-term health problems due to arthritis or a related condition [1]. The most common arthritic diseases are osteoarthritis and rheumatoid arthritis, both of which involve erosion of the cartilage cushioning the ends of bones within the joint. Symptoms include joint-pain and stiffness, which can lead to disability. Cartilage degeneration in arthritis is ultimately due to the enzymatic degradation of the cartilage extracellular matrix. The complexity and density of the cartilage extracellular matrix results in a barrier to the passage of molecules through the matrix, however its maintenance is crucial for tissue function. In the synovial joint the articular surface is lubricated and nourished by synovial fluid, a filtrate of

blood plasma containing high levels of the glycosaminoglycan hyaluronan and the proteoglycan lubricin (SZP) [2]. The relative viscosity of synovial fluid provides an additional barrier for the diffusion of molecules into chondrocytes.

Current therapies for arthritis mainly treat the clinical disease symptoms rather than targeting the degradative enzymes themselves. Treatments such as steroidal and non-steroidal anti-inflammatory drugs are still the mainstay of treatment [3,4] and can have adverse side effects including high blood pressure [5-7], osteoporosis [8], cataracts [9,10] and gastrointestinal bleeding [11]. The newly released anti-tumour necrosis factor (TNF) drugs (Etanercept, infliximab and adalimumab) which block the pro-inflammatory cytokine TNF in rheumatoid and psoriatic arthritis [12,13] are efficacious for only a small cohort of patients and are only prescribed for UK patients with severe and crippling forms of the disease as they carry the risk of serious side effects due to immuno-suppression [14].

In recent years, a number of compounds have been identified, in *in vitro* studies, that are able to inhibit the initial loss of the extracellular matrix component aggrecan, via often unknown mechanistic inhibition of the proteases ADAMTS-4 and/or -5. These compounds have notably included the nutraceutical glucosamine [14-16] and the sulphated sugar derivative pentosan polysulphate [17,18]. In addition, the physiological inhibitor of ADAMTS-4 and -5, TIMP-3, has been shown to ablate the initial loss of aggrecan in cytokine induced degradative mechanisms [19].

The idea of water-soluble polymers functioning as carriers of drugs through conjugation via a biodegradable spacer and/or linker could facilitate targeted drug release was first put forward in the mid-1970s [20]. The last two decades have seen successful clinical application of polymer conjugates to target therapeutic agents for the treatment of a range of diseases including age related macular degeneration, cancer and liver disease [21-24].

CONTACT Peter Griffiths  p.griffiths@gre.ac.uk  Department of Pharmaceutical, Chemical and Environmental Sciences, Faculty of Engineering and Science, University of Greenwich, Kent, UK

© 2017 The Author(s). Published by Informa UK Limited, trading as Taylor & Francis Group

This is an Open Access article distributed under the terms of the Creative Commons Attribution License (<http://creativecommons.org/licenses/by/4.0/>), which permits unrestricted use, distribution, and reproduction in any medium, provided the original work is properly cited.

These therapeutic conjugates have utilised a number of polymers as drug delivery vehicles including N-(2-hydroxypropyl) methacrylamide (HPMA) [25,26], poly(ethylene glycol) (PEG) [27–29] and dextrin [30,31]. Conjugation of drugs to polymers has allowed for specific targeting of the therapeutic activity of a drug to the diseased tissue. This results in a reduction of the dose required for efficacy of treatment and in potential toxicity of the drugs, respectively.

Expanding this modality to the treatment of arthritic joints, requires that such polymers in order to deliver their drug payload must be able to pass through a cartilaginous extracellular matrix rich in negatively charged proteoglycans, either to reach their chondrocytic targets or to achieve even distribution throughout the cartilage extracellular matrix. In the selection of suitable targeting polymers and polymer conjugates for the treatment of arthritic disease, quantifying whether these compounds can indeed pass through the barriers presented by the synovial joint without inducing their disruption will be of vital importance. Of the potential barriers present we believe that the interactions of polymers and polymer conjugates with proteoglycans, within the cartilage extracellular matrix as well as coating its surface, will be the most influential on their movement. This study focussed on investigating the interactions of polymers and polymer conjugates with the cartilage proteoglycans aggrecan, lubricin and synovial fluid.

Materials and methods

Preparation of synovial fluid samples

Synovial fluid samples were harvested from the metacarpo/metatarsophalangeal joints of 18 month old cows legs using a 15 gauge needle.

Preparation of lubricin

Following effusion of the synovial fluid from the joints of 18 month old cows legs as described above the joints were lavaged using 1.6M sodium chloride to isolate the lubricin coating the surface of the articular cartilage [32].

Preparation of aggrecan aggregates

Bovine articular cartilage explants were established using previous methodologies [33]. Following a 48 h preculture explants were washed into serum free DMEM. The explants were then cultured in either (i) serum free DMEM or (ii) serum free DMEM + IL-1 α (10 ng/ml). Cultures were incubated for up to 96 h; media and explants were harvested and finely diced prior to addition of guanidine extraction buffer (4 M guanidine HCl, 50 mM sodium acetate of pH 5.8–6.8, 0.1 M 6-amino-hexanoic acid, 5 mM benzamide HCl, 10 mM ethylene diamine tetra acetic acid (EDTA, tetrasodium salt), 1 mM phenyl methyl sulphonyl fluoride (PMSF-10 ml per gram cartilage wet weight) and incubated for 48 h at 4 °C with constant agitation. The extracted cartilage debris was removed by centrifugation at 15,000 rpm for 10 min and discarded. The liquid supernatant was then dialysed exhaustively against MilliQ™ water. The density of the extract was adjusted to 1.5 g/ml by addition of CaCl₂ and aggrecan-hyaluronan aggregate purified by ultracentrifugation in a Beckman L-60 Ultracentrifuge at 37,000 rpm for 70 h at 4 °C. The extract was fractionated into four equal pools designated A1–A4, the lowest fraction A1 contained the purified aggrecan-hyaluronan complex with a density >1.57 g/ml.

Analysis of cellular uptake of polymer conjugates by FACS and fluorescence microscopy

Explants were harvested and pre-cultured using previously established methods prior to incubation in the presence or absence of IL-1 α (10 ng/ml) for 96 h [34,35]. Cultures were then incubated in DMEM with 50 μ g/ml gentamicin and 10% (v/v) heat inactivated FBS in the presence or absence of Oregon Green labelled polymers at a range of concentrations (1–10 μ g/ml) for a number of time points (2–24 h). Following incubation with polymers explants were either washed in phosphate buffered saline and viewed using a confocal microscope or digested to free the cells using Pronase (1% (w/v) in DMEM containing 50 μ g/ml gentamicin and 10% (v/v) heat inactivated FBS) for 30 min at 37 °C, followed by collagenase type II (0.4% (w/v) in DMEM containing 50 μ g/ml gentamicin and 10% (v/v) heat inactivated FBS) for 45 min at 37 °C. The isolated cells was pelleted by centrifugation resuspended in PBS and run on a FACScanto (BD Biosciences, San Jose, CA).

Pulsed-gradient spin-echo nuclear magnetic resonance

Measurements on the purified freeze-dried aggrecan-hyaluronan complex re-dispersed in D₂O were conducted on a Bruker AMX360 NMR spectrometer using a stimulated echo-sequence [35]. This configuration used either a 5 mm (Cryomagnet Systems, IL) or 10 mm (Bruker) diffusion probe in conjunction with Bruker or Woodward gradient spectroscopy accessories.

The self-diffusion coefficient D_s was extracted by fitting to Equation (1) either by (i) the integrals for a given peak or (ii) the individual frequency channels present in the entire band shape via component resolved (CORE) analysis [36];

$$A(\delta, G, \Delta) = A_0 \exp[-kD_s] \quad (1)$$

where A is the signal amplitude in the absence (A_0) and presence of the field gradient pulses $A(\delta, G, \Delta)$ and $k = -\gamma^2 G^2 \left(\frac{30\Delta(\delta+\sigma)^2 - (10\delta^3 + 30\sigma\delta^2 + 35\delta^2\sigma + 14\sigma^3)^2}{30} \right)$ given that γ is the magnetogyric ratio, Δ the diffusion time, σ the gradient ramp time, δ the gradient pulse length and G the gradient field strength.

Small-angle neutron scattering

SANS experiments were performed on the LOQ diffractometer based at the spallation source at the Rutherford Appleton Laboratory, UK, where a Q range of 0.007 to 0.3 \AA^{-1} is accessible using $2 < \lambda < 10 \text{\AA}$, where $Q = (4\pi/\lambda)\sin(\theta/2) = \left(\frac{q}{\lambda}\right)\sin\left(\frac{\theta}{2}\right)$.

Samples were contained in 1 mm pathlength, UV-spectrophotometer grade, quartz cuvettes (Hellma) and mounted in aluminium holders on top of an enclosed, computer-controlled, sample chamber. Temperature control was achieved through the use of a thermostatted circulating bath pumping fluid through the base of the sample chamber. Under these conditions a temperature stability of better than ± 0.5 °C can be achieved. Experimental measuring times were approximately 40–60 min.

All scattering data were normalised for the sample transmission and the incident wavelength distribution was corrected for instrumental and sample backgrounds using a quartz cell filled with either H₂O or D₂O (this also removes the incoherent instrumental background arising from vacuum windows, etc.) and corrected for the linearity and efficiency of the detector response using the instrument specific software package (e.g. Mantid). The data were put onto an absolute scale using a well-characterised partially deuterated polystyrene blend standard sample.

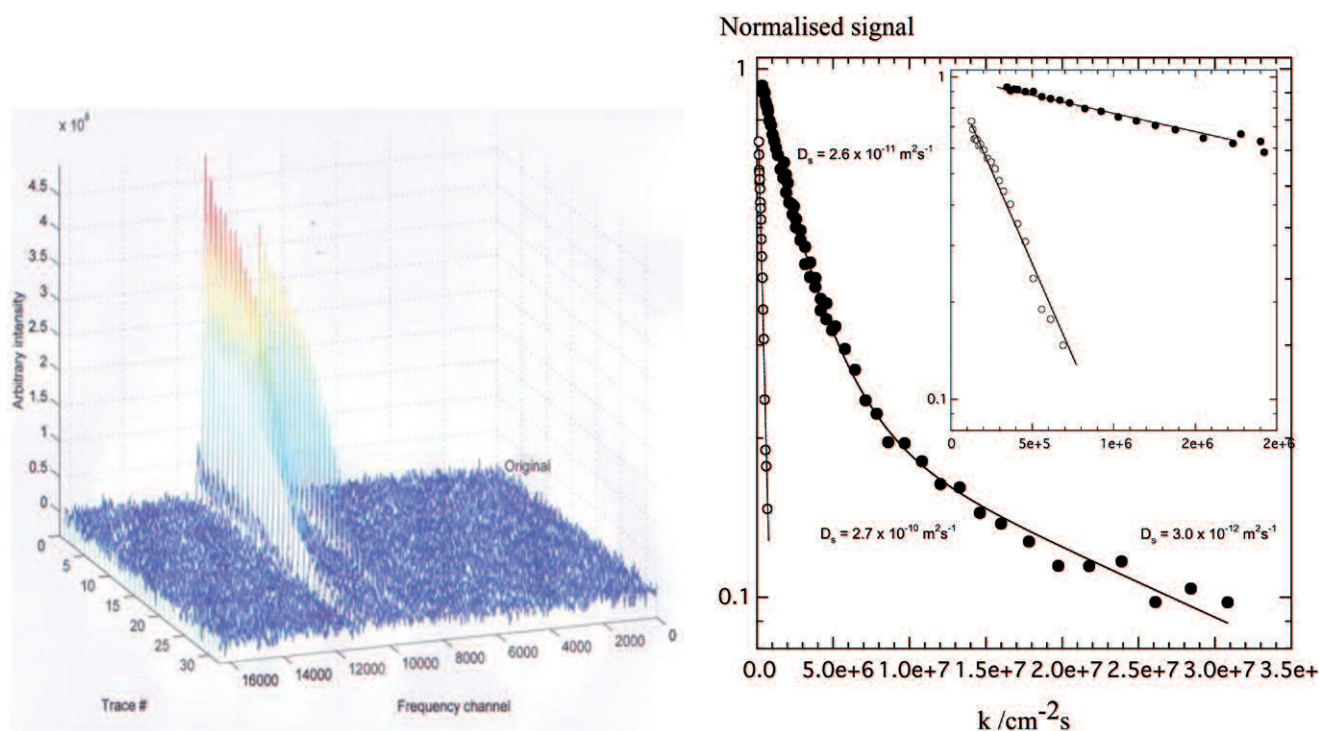


Figure 1. Experimental two-dimensional PGSE NMR dataset (left) and analysis of peak integrals used to extract the rates of diffusion (right) for $M_w = 10 \text{ kg mol}^{-1}$ dextrin in free solution and in an aggrecan-hyaluronan gel, the open symbols correspond to the attenuation function for the peak at $\sim 3 \text{ ppm}$ in the spectrum from 10 mg/ml (1 wt\%) dextrin in solution i.e. the raw data presented above. The filled symbols correspond to two superimposed datasets, necessary to span the wide dynamics range present in these systems, again for the 3 ppm peak, arising from the spectrum of 10 mg/ml (1 wt\%) dextrin in an aggrecan-hyaluronan gel (20 mg/ml GAG).

The intensity of the scattered radiation, $I(Q)$, as a function of the wavevector, is given by:

$$I(Q) = NV^2(\Delta\rho)^2P(Q)S(Q) + B_{inc} \quad (2)$$

where $P(Q)$ describes the morphology of the scattering species, $S(Q)$ describes the spatial arrangement of the species in solution, N is the number of species per unit volume, V is the volume of the species, $\Delta\rho$ is the difference in the neutron scattering length density (SLD) of the scatterer and the solvent and B_{inc} is the incoherent background scattering.

Results and discussion

Pulsed gradient spin echo nuclear-magnetic resonance spectroscopy (PGSE-NMR) provides a convenient and non-invasive chemically selective technique for measuring translational motion and in particular the self-, rather than mutual-diffusion coefficient. Therefore, PGSE-NMR can be used both to quantify the mobility of molecules and to assess the impact of the presence of the molecules on the extracellular matrix components themselves. The diffusion of small solutes (including water and Na^+) has been shown to be impeded by up to 40% by the presence of an extracellular matrix, implying that the movement of larger molecules such as polymers may be very significantly affected by the presence of a matrix [37].

A vital component in the selection of polymer-drug conjugates for the treatment of arthritic disease is the selection of either polymers which are able to target a drug with intracellular activity and its ability to diffuse rapidly through the extracellular matrix into the chondrocyte. Accordingly, the rate of diffusion of dextrin polymers (as model conjugates) has been quantified both in free solution and through components of the cartilaginous extracellular

Table 1. Self-diffusion coefficients in free solution (concentration 1 wt\%) and aggrecan-hyaluronan gels measured by PGSE-NMR and the retardation ratio from free solution to gel.

Sample	Free solution	Aggrecan-hyaluronan	Ratio
$M_w = 10 \text{ kg mol}^{-1}$	$2.7 \times 10^{-10} \text{ m}^2 \text{ s}^{-1}$	$2.6 \times 10^{-11} \text{ m}^2 \text{ s}^{-1}$	10
$M_w = 51 \text{ kg mol}^{-1}$	$1.0 \times 10^{-10} \text{ m}^2 \text{ s}^{-1}$	$5.0 \times 10^{-12} \text{ m}^2 \text{ s}^{-1}$	20

matrix (Figure 1). The matrix comprises an aggrecan-hyaluronan aggregate gel purified by density gradient centrifugation from bovine articular cartilage, is presented in Table 1. For the $M_w = 10 \text{ kg mol}^{-1}$ dextrin sample, the self-diffusion coefficient was slowed from $D_s = 2.7 \times 10^{-10} \text{ m}^2 \text{ s}^{-1}$ in free solution, corresponding to a hydrodynamic radius of a few nanometres, to $D_s = 2.6 \times 10^{-11} \text{ m}^2 \text{ s}^{-1}$ in the aggrecan-hyaluronan gel (Table 1). The higher molecular weight dextrin shows a larger reduction, though the free solution retardation is consistent with the increase in molecular weight of a random coil configuration. By drawing analogies of the diffusion of such a polymer in related (mucin) gels, this significant retardation is probably not a consequence of direct association of the dextrin with the aggrecan-hyaluronan aggregate, but rather steric hindrance due to the presence of the highly entangled matrix of the aggrecan-hyaluronan aggregate [38]. The non-linearity of the attenuation function clearly demonstrates the presence of more than a single diffusion rate and the CORE analysis identifies these to be dextrin (the initial decay) and the underlying much slower (two orders of magnitude slower) diffusion of the aggrecan-hyaluronan aggregates.

On the other side, we can also comment on the effect of succinylation, which is the first step in dextrin functionalisation – on the conformation of the polymer, as characterised by their self-diffusion coefficients (Figure 2). The self-diffusion coefficient drops smoothly (increasing hydrodynamic size) with increasing mole

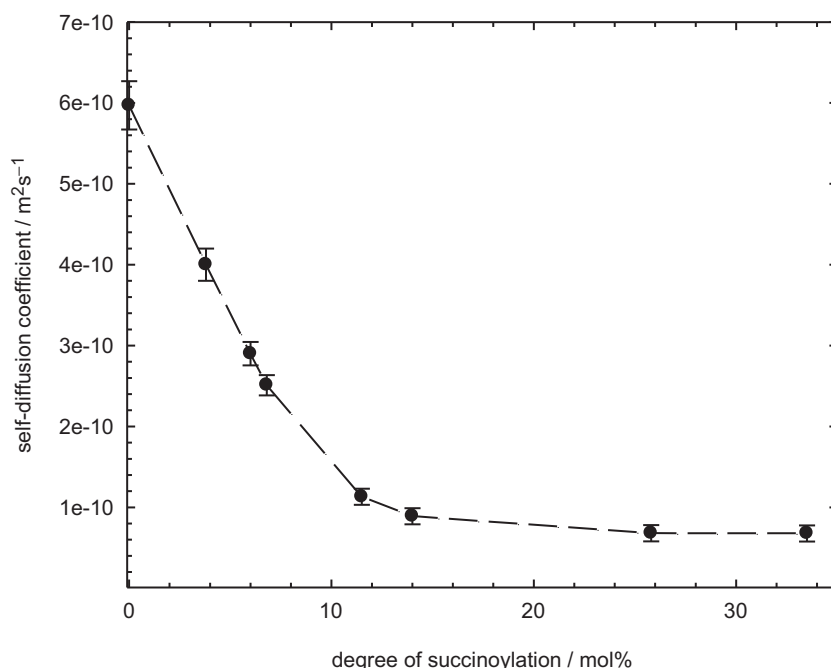


Figure 2. Self-diffusion coefficients in free solution as a function of degree of succinylation measured by PGSE-NMR for dextrin $M_w = 51 \text{ kg mol}^{-1}$ at 1 wt% polymer.

percent of succinylation, up to a value of around $\sim 10 \text{ mol}\%$, above which the self-diffusion coefficient becomes largely constant at $\sim 1 \times 10^{-10} \text{ m}^2 \text{ s}^{-1}$, consistent with an hydrodynamic radius of around 50 \AA .

The (gel) structure of cartilage extract and various derivative materials have been examined based on Beaucage model by small-angle neutron scattering (SANS) in the absence and presence of added dextrin, as shown in Figure 3(a,b) (representative data only presented). In the case of the 18 m direct cartilage extract, where the scattering from the gel itself is significant ($I(Q) > 10 \text{ cm}^{-1}$ at $Q < 0.01 \text{ \AA}^{-1}$) and dominates the mixture scattering (for dextrin, $I(Q) < 0.5 \text{ cm}^{-1}$ at $Q < 0.01 \text{ \AA}^{-1}$), addition of the two dextrin samples induced no noticeable perturbation in the scattering and hence, structure of the direct cartilage extract gel. In the case of the IL-1 systems and various other derivative materials (data not presented, Figure 3(b)), the same conclusion may be drawn, but not so directly. It is obvious that the scattering does vary across the different mixed systems, but it is shown below that this is a consequence of the weaker and comparable intensities of the various components rather than one dominating contribution, as in the case of the 18 m direct cartilage extract.

A number of strategies exist for interpreting SANS data. The simplest is to consider the slope of the data when plotted on a double logarithmic representation, extracting the so-called Q dependency, $I(Q) \propto Q^{-n}$, illustrating the most probable shape of the scatterer; $n = 1$ indicates a rod, $n = 2$ a flat structure, increasing all the way to $n = 4$ for a large, solid object. For systems like gels, one might anticipate $n = 5/3$ to the $n = 3$, reflecting a transition from a mass to volume fractal character associated with the differing length-scales present in the gel. This is indeed the case.

Alternatively, one may numerically analyse the data in terms of specific models, based on some *a priori* knowledge of the likely conformation or arrangement of molecules in solution. For dextrin, a simple polydisperse Gaussian coil model adequately describes the data for $M_w = 51 \text{ kg mol}^{-1}$ dextrin sample, with $R_G = 80 \text{ \AA}$

(consistent with the theoretical prediction for the ratio of the radius of gyration and hydrodynamic radius, $R_G/R_H = 1.5$).

For the gels, an appropriate treatment is the Shibayama-Geissler two-length scale model [39,40] which treats the scattering as the additional of two components, with fraction f ;

$$I(Q) = fI(0)_1 \frac{1}{\left(1 + \left(\frac{D+1}{3}\right)Q^2 a_1^2\right)^{D/2}} + (1-f)I(0)_2 \exp(-Q^2 a_2^2) + B \quad (3)$$

where D is the scaling exponent and $a_2^2 \approx \frac{R_G^2}{3}$. The parameters describing the Shibayama-Geissler fit to these data are presented in Table 2. By and large, the fitting is most sensitive to the Lorentzian component embodied in the scaling exponent D , with a length scale (a_1^2) of around 100 \AA , but the 18 m direct cartilage extract also requires a Guinier term, with length scale slightly shorter. Most importantly, as is evident from the raw data where subtle differences are only observed at higher Q values, the parameters are largely insensitive to the addition of the dextrin i.e. it may be considered to be non-perturbing.

Having shown it is possible for dextrin to diffuse through the gel whilst having little impact on its structure, the progression of (Oregon Green labelled) dextrin into chondrocytes was assessed. Each of the cultures was incubated in dextrin-Oregon Green at 1, 5 and $10 \mu\text{g/ml}$ for 2–24 h, respectively. Cells were released from monolayer cultures by gentle trypsinisation and by rapid pronase and collagenase digest from explant and *ex vivo* transwell grafts cultures. FACS analysis of these cell populations with $10 \mu\text{g/ml}$ dextrin-Oregon Green at 2, 4, 8 and 24 h are shown in Figure 4.

Cellular uptake of the dextrin conjugate achieved in the presence of a cartilaginous extracellular matrix in both explant cultures and in *ex vivo* transwell grafts is shown in Figure 4(a,b), respectively. In cartilage explants cellular uptake was achieved in over 90% of cells following 8 h exposure (Figure 4(b)). Uptake of dextrin-Oregon Green was slower in *ex vivo* transwell grafts than in explants cultures with only 66% of cells containing the

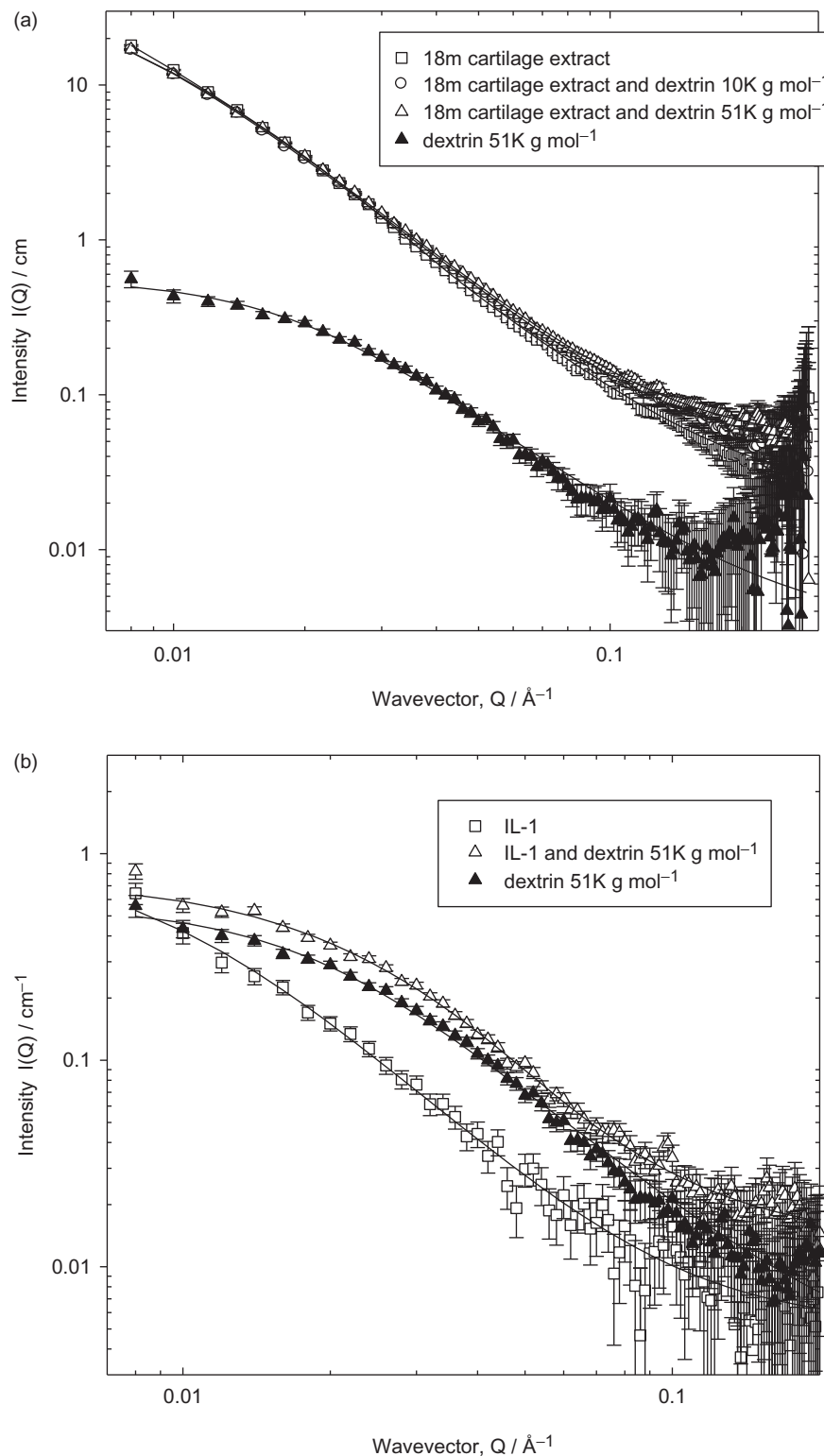


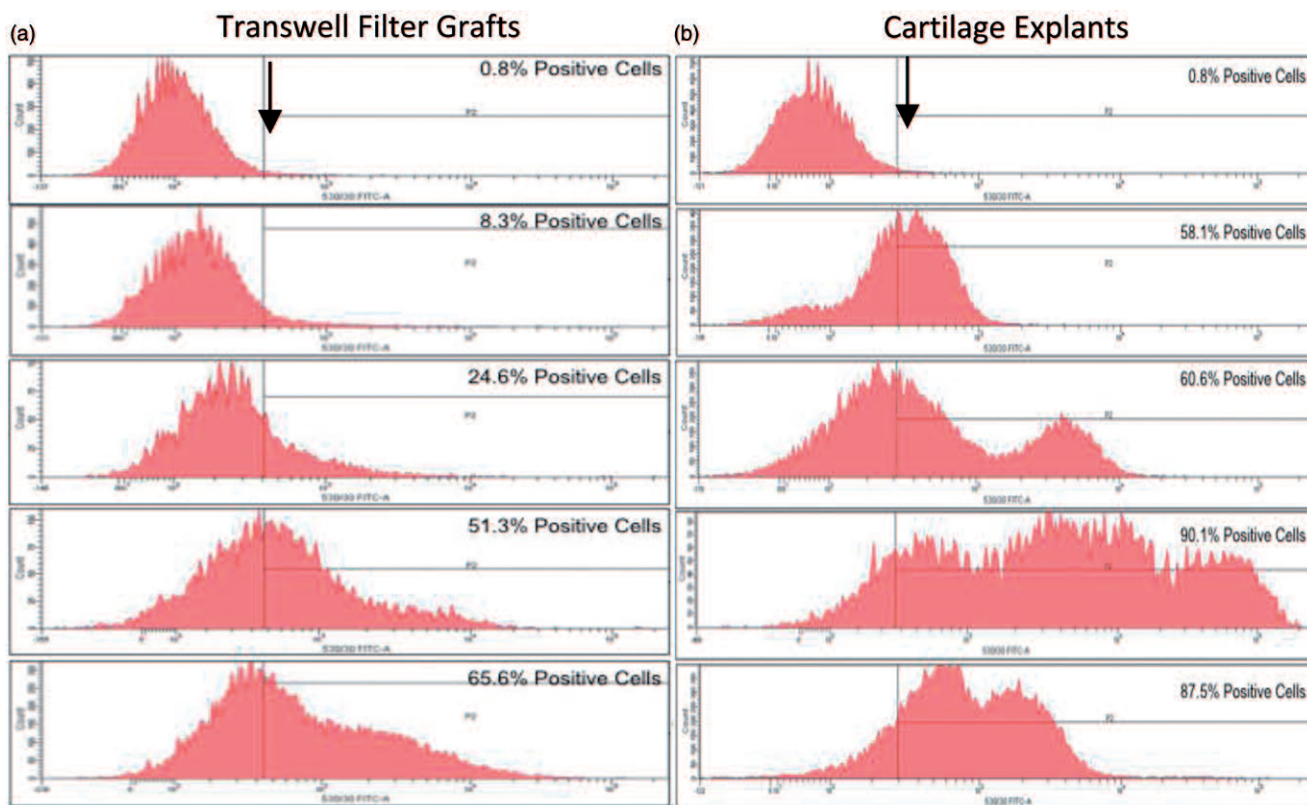
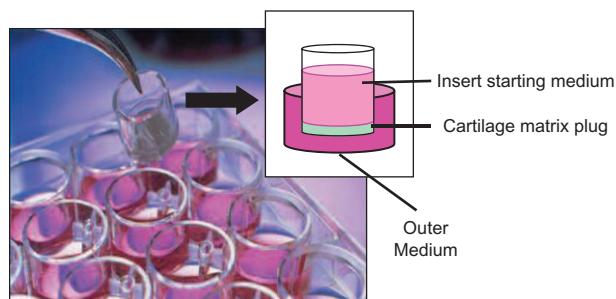
Figure 3. (a) Small-angle neutron scattering from 1 mm thick (H_2O) aqueous solutions of direct cartilage extract from 18 month old knee joints in the absence of dextrin and in the presence of 1 wt% dextrin, $M_w = 10$ and 51 kg mol^{-1} , respectively. The lines of best fit have been derived from the analysis using the Beaucage model as described in the text. Also shown for comparison is the scattering from 1 wt% $M_w = 51 \text{ kg mol}^{-1}$ dextrin (in D_2O). The lines of best fit for this dextrin sample has been derived from a simple Gaussian coil model, $R_G = 80 (\pm 3) \text{ \AA}$. (b) Small-angle neutron scattering from 2 mm thick (D_2O) reconstituted aqueous solutions of IL-1 in the absence of dextrin and in the presence of 1 wt% dextrin $M_w = 51 \text{ kg mol}^{-1}$. The lines of best fit have been derived from the analysis using the gel plus coil model as described in the text. Also shown for comparison is the scattering from the dextrin solution.

fluorophore following 24 h exposure (Figure 4(a)). In the *ex vivo* transwell grafts the dextrin-Oregon Green was only added to the insert medium to mimic the situation *in vivo* where a therapeutic agent injected into the joint would only be able to penetrate the

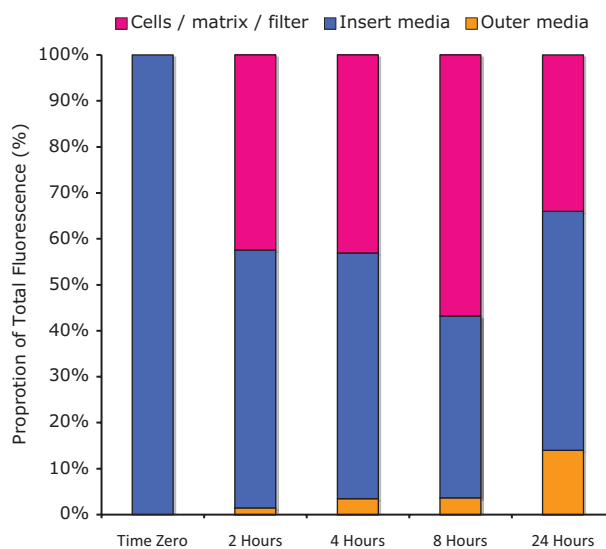
cartilage at the articular surface (Figure 5). This restricted access to one surface explains the apparently slower rate of uptake by chondrocytes within the *ex vivo* transwell grafts compared to chondrocytes within cartilage explants (Figure 4(a,b)).

Table 2. Parameters derived from an analysis of the scattering data in terms of the Shibayama-Geissler two-length scale model.

Sample	Guinier scale	Lorentzian scale	Radius of gyration(Å)	Fractal dimension	Correlation length(Å)
18 m	0.2	18	85 ((+/- 3)	2.2 ((+/- 0.1)	235 ((+/- 30)
18 m plus dextrin 10 kg mol ⁻¹	n/a	18	n/a	2.3	140
18 m plus dextrin 51 kg mol ⁻¹	n/a	14	n/a	2.3	135
IL-1	n/a	0.2	n/a	2.2	105
IL-1 plus dextrin 51 kg mol ⁻¹	0.3	1.1	55	2.2	90

**Figure 4.** FACS analysis of dextrin-Oregon Green uptake with time in: (a) chondrocytes isolated from *ex vivo* transwell grafts following exposure to dextrin-Oregon Green and (b) chondrocytes isolated from articular cartilage explants cultures following exposure to dextrin-Oregon Green.**Figure 5.** Picture of *ex vivo* transwell grafts and diagrammatic representation of the structure of the cultures (insert).

In order to determine whether dextrin-Oregon Green was able to pass right through a cartilaginous extracellular matrix it was only added to the insert medium of the *ex vivo* transwell grafts and both the insert and outer medium were analysed for its presence using fluorescence spectroscopy following a number of different incubation times (Figure 6). It is tacitly assumed, as shown in other studies, that the Oregon Green remains attached to the dextrin [41].

**Figure 6.** Analysis of the distribution of fluorescence in transwell filter cultures by fluorescence spectroscopy.

The dextrin-Oregon Green was able to pass right through the extracellular matrix of the *ex vivo* transwell grafts and was detected in the outer medium of the cultures following only 2 h of incubation with the conjugate (Figure 6). Following 24 h incubation on the filter insert cultures over 13% of the total fluorescence present in the cultures was detected in the outer medium (Figure 6).

Conclusions

Combined, the data presented here demonstrate that dextrin is able to successfully diffuse through a cartilaginous extracellular matrix and into the chondrocytes within, inducing little perturbation in that matrix, thus indicating the feasibility of drug delivery using polymer conjugates for the treatment of arthritis.

Disclosure statement

None of the authors has received any financial interest or benefit that has arisen from the direct applications of our research.

Funding

This work was supported by Engineering and Physical Sciences Research Council under Platform Grant (EP/C013220/1) "Bioresponsive polymer therapeutics; synthesis and characterisation of novel nanomedicines".

References

- [1] Working with Arthritis, Arthritis Research UK, June 2016. Available from: <http://www.arthritisresearchuk.org/policy-and-public-affairs/reports-and-resources/reports/work-report.aspx>.
- [2] Rhee DK, Marcelino J, Baker M, et al. The secreted glycoprotein lubricin protects cartilage surfaces and inhibits synovial cell overgrowth. *J Clin Invest*. 2005;115:622–631.
- [3] Marini S, Fasciglione GF, Monteleone G, et al. A correlation between knee cartilage degradation observed by arthroscopy and synovial proteinases activities. *Clin Biochem*. 2003;36:295–304.
- [4] Brandt KD, Slowman-Kovacs S. Nonsteroidal anti-inflammatory drugs in treatment of osteoarthritis. *Clin Orthop*. 1986;213:84–91.
- [5] Gabriel SE, Wagner JL. Costs and effectiveness of nonsteroidal anti-inflammatory drugs: the importance of reducing side effects. *Arthritis Care Res*. 1997;10:56–63.
- [6] Hammer F, Stewart PM. Cortisol metabolism in hypertension. *Best Pract Res Clin Endocrinol Metab*. 2006;20:337–353.
- [7] Reiche ML. Complications of intravitreal steroid injections. *Clin Care*. 2005;76:450–460.
- [8] Ledford D, Apter A, Brenner AM, et al. Osteoporosis in the corticosteroid treated patient with asthma. *J Allergy Clin Immunol*. 1998;102:353–363.
- [9] Moore P. Inhaled corticosteroids increase cataract risk. *Lancet*. 1997;350:120.
- [10] Urban RC, Cotlier E. Corticosteroid-induced cataracts. *Surv Ophthalmol*. 1986;31:102–110.
- [11] Tringham VM, Cochrane P. Aspirin, paracetamol, diflunisal, and gastrointestinal blood-loss. *Lancet*. 1979;1:1409.
- [12] Punzi L, Podswiadek M, Sfriso P, et al. Pathogenic and clinical rationale for TNF-blocking therapy in psoriatic arthritis. *Autoimmun Rev*. 2007;6:524–528.
- [13] Berthelot J-M, Varin S, Cormier G, et al. 25 mg etanercept once weekly in rheumatoid arthritis and spondylarthropathy. *Joint Bone Spine*. 2007;74:144–147.
- [14] Maillard H, Ornetti P, Grimault L, et al. Severe pyogenic infections in patients taking infliximab: a regional cohort study. *Joint Bone Spine*. 2005;72:330–334.
- [15] Largo R, Alvarez-Soria MA, Diez-Ortego I, et al. Glucosamine inhibits IL-1beta-induced NFkappaB activation in human osteoarthritic chondrocytes. *Osteoarthritis Cartilage*. 2003;11:290–298.
- [16] Ilic MZ, Martinac B, Handley CJ. Effects of long-term exposure to glucosamine and mannosamine on aggrecan degradation in articular cartilage. *Osteoarthritis Cartilage*. 2003;11:1–10.
- [17] Smith JG, Hannon RL, Brunnberg L, et al. A multicentre clinical study of the efficacy of sodium pentosan polysulphate and carprofen in canine osteoarthritis. *Norsk Veterinaertidsskrift*. 2002;123–130.
- [18] Rogachefsky RA, Dean DD, Howell DS, et al. Treatment of canine osteoarthritis with sodium pentosan polysulphate and insulin-like growth factor-1. *Ann N Y Acad Sci*. 1994;732:392–394.
- [19] Gendron C, Kashiwagi M, Hughes CE, et al. TIMP-3 inhibits aggrecanase-mediated glycosaminoglycan release from cartilage explants stimulated by catabolic factors. *FEBS Letters*. 2003;555:431–436.
- [20] Vasey PA, Kaye SB, Morrison R, et al. Phase I Clinical and pharmacokinetic study of PK1 [N-(2-hydroxypropyl) methacrylamide copolymer doxorubicin]: first member of a new class of chemotherapeutic agents- drug-polymer conjugates. *Clin Cancer Res*. 1999;5:83–94.
- [21] Duncan R. Targeting and intracellular delivery of drugs. In: Meyers RA, editor. *Encyclopedia of molecular cell biology and molecular medicine*. Weinheim, Germany: Wiley-VCH, Verlag, GmbH & Co; 2005. p.163–204.
- [22] Duncan R. Polymer conjugates as anticancer nanomedicines. *Nat Rev Cancer*. 2006;6:688–701.
- [23] Duncan R, Ringsdorf H, Satchi-Fainaro R. Polymer therapeutics, polymers as drugs, conjugates and gene delivery systems: past, present and future opportunities. *Adv Polym Sci*. 2006;192:1–8.
- [24] Yasukawa T, Ogura Y, Sakurai E, et al. Intraocular sustained drug delivery using implantable polymeric devices. *Adv Drug Deliv Rev*. 2005;57:2033–2046.
- [25] Duncan R, Vicent MJ, Greco F, et al. Polymer-drug conjugates: towards a novel approach for the treatment of endocrine-related cancer. *Endocr Relat Cancer*. 2005;12:189–199.
- [26] Nan A, Nanayakkara NPD, Walker LA, et al. N-(2-hydroxypropyl)methacrylamide (HPMA) copolymers for targeted delivery of 8-aminoquinoline antileishmanial drugs. *J Control Release*. 2001;77:233–243.
- [27] Ould-Ouali L, Noppe M, Langlois X, et al. Self-assembling PEG- ρ (CL-co-TMC) copolymers for oral delivery of poorly water soluble drugs: a case study with risperidone. *J Control Release*. 2005;102:657–668.
- [28] Cheng J, Tepy BA, Sherifi I, et al. Formulation of functionalized PLGA-PEG nanoparticles for in vivo targeted drug delivery. *Biomaterials*. 2007;28:869–876.
- [29] Yu D, Peng P, Dharap SS, et al. Antitumor activity of poly(ethylene glycol)-camptothecin conjugate: The inhibition of tumor growth in vivo. *J Control Release*. 2005;110:90–102.

- [30] Hreczuk-Hirst D, Chicco D, German L, et al. Dextrins as potential carriers for drug targeting: tailored rates of dextrin degradation by introduction of pendant group. *Int J Pharm.* 2001;230:57–66.
- [31] Hreczuk-Hirst D, German L, Duncan R. Dextrins as carriers for drug targeting: reproducible succinylation as a means to introduce pendant groups. *J Bioact Compat Polym.* 2001; 16:353–364.
- [32] Jones ARC, Gleghorn JP, Hughes CE, et al. Binding and localization of recombinant lubricin to articular cartilage surfaces. *J Orthop Res.* 2007;25:283–292.
- [33] Hughes CE, Caterson B, Fosang AJ, et al. Monoclonal antibodies that specifically recognise neopeptide sequences generated by aggrecanases and matrix metalloproteinase cleavage of aggrecan: application to catabolism in situ and in vitro. *Biochem J.* 1995;305:799–804.
- [34] Arner EC, Hughes CE, Decicco CP, et al. Cytokine-induced cartilage proteoglycan degradation is mediated by aggrecanase. *Osteoarthritis Cartilage.* 1998;6:214–228.
- [35] Davies JA, Griffiths PC. A phenomenological approach to separating the effects of obstruction and binding for the diffusion of small molecules in polymer solutions. *Macromolecules.* 2003;36:950.
- [36] Stilbs P, Paulsen K, Griffiths PC. Global least-squares analysis of large, correlated spectral data sets: application to component-resolved FT-PGSE NMR spectroscopy. *J Phys Chem.* 1996;100:8180–8189.
- [37] Burstein D, Gray ML, Hartman AL, et al. Diffusion of small solutes in cartilage as measured by nuclear magnetic resonance (NMR) spectroscopy and imaging. *J Orthop Res.* 1993;11:465–478.
- [38] Griffiths PC, Occhipinti P, Gumbleton M, et al. PGSE-NMR and SANS Studies of the interaction of model polymer therapeutics with mucin. *Biomacromolecules.* 2010;11:120–125.
- [39] Shibayama M, Toyochi T, Han CC. Small angle neutron scattering study on poly(N-isopropyl acrylamide) gels near their volume-phase transition temperature. *J Chem Phys.* 1992; 97:6829–6841.
- [40] Mallam S, Horkay F, Hecht AM, et al. Microscopic and macroscopic thermodynamic observations in swollen poly(dimethylsiloxane) networks. *Macromolecules.* 1991;24:543.
- [41] Richardson SC, Wallom KL, Ferguson EL, et al. The use of fluorescence microscopy to define polymer localisation to the late endocytic compartments in cells that are targets for drug delivery. *J Control Release.* 2008;127:1–11.